

Accepted Manuscript

BODIPY based fluorescent turn-on sensor for highly selective detection of HNO and the application in living cells

Xiaolong Zhao, Chao Gao, Na Li, Fayu Liu, Shuhui Huo, Jianzhen Li, Xiaolin Guan, Na Yan

PII: S0040-4039(19)30410-1
DOI: <https://doi.org/10.1016/j.tetlet.2019.04.049>
Reference: TETL 50764

To appear in: *Tetrahedron Letters*

Received Date: 27 February 2019
Revised Date: 17 April 2019
Accepted Date: 28 April 2019

Please cite this article as: Zhao, X., Gao, C., Li, N., Liu, F., Huo, S., Li, J., Guan, X., Yan, N., BODIPY based fluorescent turn-on sensor for highly selective detection of HNO and the application in living cells, *Tetrahedron Letters* (2019), doi: <https://doi.org/10.1016/j.tetlet.2019.04.049>

This is a PDF file of an unedited manuscript that has been accepted for publication. As a service to our customers we are providing this early version of the manuscript. The manuscript will undergo copyediting, typesetting, and review of the resulting proof before it is published in its final form. Please note that during the production process errors may be discovered which could affect the content, and all legal disclaimers that apply to the journal pertain.



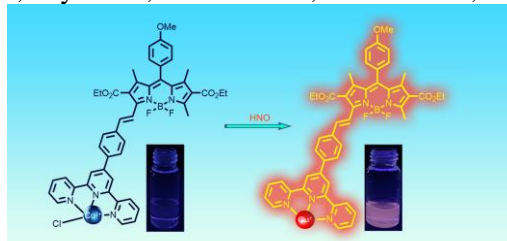
Graphical Abstract

To create your abstract, type over the instructions in the template box below.
Fonts or abstract dimensions should not be changed or altered.

Bodipy based fluorescent turn-on sensor for highly selective detection of HNO and the application in living cells

Xiaolong Zhao^a, Chao Gao^a, Na Li^a, Fayu Liu^a, Shuhui Huo^a, Jianzhen Li^b, Xiaolin Guan^a, Na Yan^c

Leave this area blank for abstract info.





BODIPY based fluorescent turn-on sensor for highly selective detection of HNO and the application in living cells

Xiaolong Zhao^{a, *}, Chao Gao^a, Na Li^a, Fayu Liu^a, Shuhui Huo^a, Jianzhen Li^b, Xiaolin Guan^a, Na Yan^{c, *}

^a Key Laboratory of Eco-Environment-Related Polymer Materials, Ministry of Education, College of Chemistry and Chemical Engineering, Northwest Normal University, Lanzhou, Gansu 730070, P. R. China

^b College of Life Sciences, Northwest Normal University, Lanzhou, Gansu 730070, P. R. China

^c School of Pharmacy, Lanzhou University, Lanzhou 730000, P. R. China

ARTICLE INFO

Article history:

Received

Received in revised form

Accepted

Available online

Keywords:

Synthesis

BODIPY Sensors

Fluorescent Turn-on

HNO Detection

Bioimaging

ABSTRACT

On the basis of BODIPY platform, a terpyridyl-substituent BODIPY-Copper complex (Cu(II)-BTPY) was rationally designed and synthesized as a redox reaction fluorescent sensor for detecting HNO over reactive oxygen species (ROS) and reactive nitrogen species (RNS) with impressive selectivity in living cells under mild and neutral conditions. The BTPY exhibits relatively high fluorescence quantum efficiency as much as 34.8% and presents large Stokes shift, about 62 nm. When a series of transition metal ions were exploited to investigate the fluorescence quench towards BTPY, copper ion (Cu²⁺) gave the optimal result. After the fluorescence of the probe being effectively quenched in the presence of Cu²⁺, it can be in turn recovered through the reduction of Cu²⁺ into Cu⁺ by HNO accompanying with a visually observable fluorescence response. Still, the sensing mechanism was evidently confirmed by EPR and ESI-MS measurement. In addition, the employment of BTPY for imaging dyes was also presented in vivo.

2009 Elsevier Ltd. All rights reserved.

Introduction

Nitric oxide (NO), a powerful necrotic agent wielded by macrophages of the immune system, plays an important role in physiological and pathological processes.¹ As a single electron reduction product of nitric oxide, nitrosyl hydrogen (HNO) significantly displays biological performance with potential pharmacological applications.² Mutually, NO and HNO may be able to convert into each other in the presence of superoxide dismutase (SOD), while the biological nature of the nitrosyl hydrogen is not exactly the same as nitric oxide.³ Unlike NO, HNO has a positive inotropic effect and a lipophilic effect with independent signal channel to β -adrenalin stimulation.⁴ Besides, HNO has an apparent effect on the ryanodine receptor, micromolar concentrations of HNO will help protect the heart's function.⁵ Currently, studies on the biological applications, however, are still hindered by lacks in sensitivity, specificity, and real-time detection as well as direct observation.⁶ Traditional method mainly aims at detecting the HNO by-products, such as HNO dehydrated creature, nitrous oxide, capable of being determined via headspace gas chromatography, UV-visible (UV),

¹H NMR, and electron paramagnetic resonance (EPR).⁷ Though some of the finely designed probes have been employed to evaluate HNO in biological processes, yet precise identification of HNO in vivo is confined by the short of suitable probes using fluorescence turn-on signals rather than turn-off signals.⁸ One alternative strategy to achieve fluorescence turn-on involves the employment of reaction-based organic fluorescent chemodosimeter, an indicator grounded on the fluorescence-quenched metal complex, in which the coordinated metal would be reduced by HNO, and subsequently restored the fluorescence of the probe.⁹

Boron-dipyrromethene (BODIPY) derivatives, similar to other fluorescent dyes,¹⁰ have been widely studied. They favor properties including high fluorescence quantum efficiency, large molar extinction coefficient, relatively long excited state lifetimes as well as chemical/light robustness, and therefore has been used as luminescent devices, chemical sensors, and molecular wires.¹¹ Besides, in the field of biological labeling, BODIPY dyes also act as promising candidates for small biological molecules detection in vivo and organism imagine.¹²

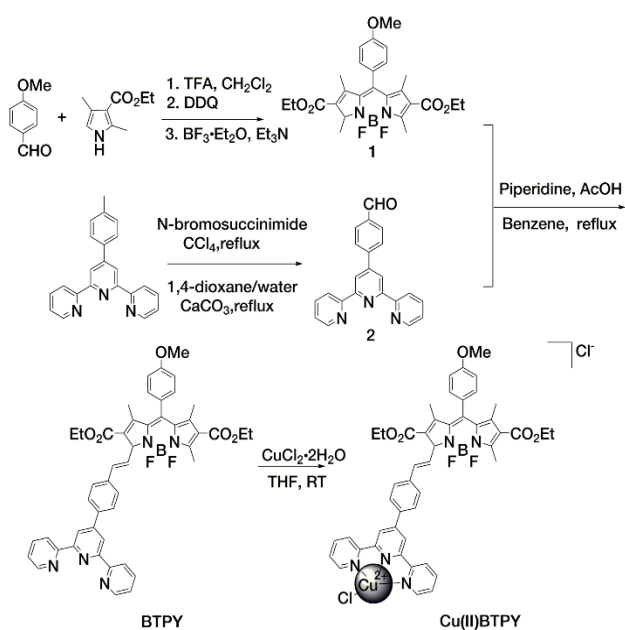
* Corresponding author. E-mail: zhaoxl82@nwnu.edu.cn

Thanks to its accessible modification for the molecular structure, diverse substituents at different position were actualized to give various properties. Extending the π -conjugation framework at 3-, 5- and 8-positions might bring about red-shifted absorption and emission, while alkylation of 1, 7-positions may render the materials with large Stokes shifts.¹³ To the best of our knowledge, small Stokes shift probably limits high sensitivity imaging *in vivo* since it can be simply disturbed by biological background.¹⁴

Herein, we report a BODIPY fluorescent sensor possessing large Stokes shift for the purpose of developing a method capable of quickly *in situ* detecting HNO₃ via fluorescence turn-on mode. Given that electrophilic reactions may easily take place in absence of substituent at 2, 6-positions due to the increment of electron cloud density, two esters were first introduced at 2, 6-positions in the framework of the sensor. Successively, one 4-methoxyphenyl substituent occupied the 8-position while two methyl groups took the 1, 7 positions so as to cooperatively hamper the free rotation of the BODIPY skeleton, and therefore gave an impressively enhanced Stokes shift.¹⁵ Additionally, a terpyridyl-substituent styryl group was presented at position 3 to proffer a heterocyclic tridentate ligand in possession of a strongly conjugating ability derived from the aromatic rings, and resultantly be able to easily coordinate with transition metals.¹⁶ Playing the role as a paramagnetic fluorescence complex, the prepared **Cu(II)-BTPY** exhibits the turn-off fluorescence (Scheme 1). Conversely, the fluorescence can be recovered accompanying with the reduction of Cu(II) into Cu(I), in which photo-induced electron transfer (PET) is destroyed by the diamagnetic Cu(I)-BTPY.¹⁷

Results and discussion

As shown in Scheme 1, **Cu(II)-BTPY** is readily synthesized from pyrrole derivatives. 2, 4-Dimethyl-3-carboxylic acid ethyl ester pyrrole was treated with anisaldehyde in the presence of a catalytic amount of trifluoroacetic acid (TFA) under nitrogen atmosphere. Afterwards, BODIPY **1** was obtained as a secondary product via the oxidative dehydrogenation with 18% yield. Compound **3**, prepared from **2** according to previous report, was involved in Knoevenagel reaction to condense with **1** and



Scheme 1. Synthetic of **Cu(II)-BTPY**.

engender the **BTPY** in presence of acetic acid and piperidine while keeping refluxing.¹⁸

The **BTPY**, a typical BODIPY chromophore, exhibits obvious Stokes shift (62 nm) and displays optical properties with an absorption band in the visible region. After respectively adding Zn²⁺, Rh³⁺, Cd²⁺, Pb²⁺, Ca²⁺, Ni²⁺, Ba²⁺, Mn²⁺, Au³⁺, Hg²⁺, Fe³⁺, Al³⁺, Ag⁺ and Cr³⁺, their fluorescence intensity were insignificantly changed. In contrast, fluorescence intensity greatly decreased after adding Co²⁺ or Cu²⁺, giving 39.8% or 4.6% compared to that of **BTPY**, respectively (Fig. 1). The fluorescence response reveals a special selectivity towards Cu²⁺ other than that of other metals, i. e., Co²⁺, Zn²⁺, Rh³⁺, Cd²⁺, Pb²⁺,

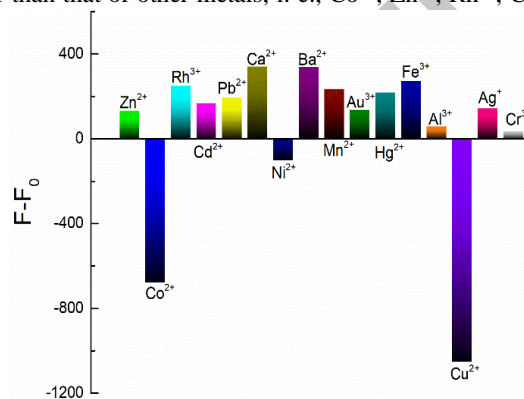


Fig. 1. Fluorescence response of **BTPY** (1 μ M) to the addition of different metal ions (10 μ M) of Cu²⁺, Co²⁺, Zn²⁺, Rh³⁺, Cd²⁺, Pb²⁺, Ca²⁺, Ni²⁺, Ba²⁺, Mn²⁺, Au³⁺, Hg²⁺, Fe³⁺, Al³⁺, Ag⁺ and Cr³⁺ in THF. F represents the maximum fluorescence intensity of the **BTPY** after adding different metal ions, and F₀ represents the initial fluorescence intensity of **BTPY**.

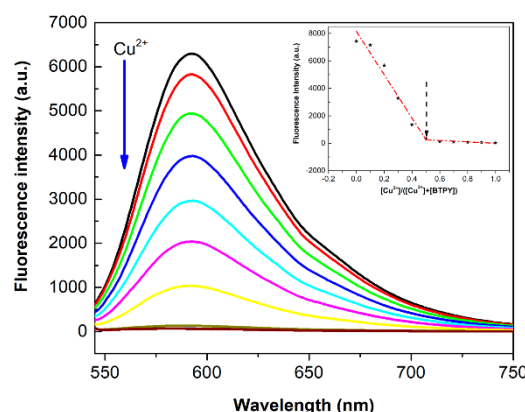


Fig. 2. Changes in fluorescence spectra of **BTPY** (10 μ M) upon incremental addition Cu²⁺ ion (0 -1.0 equivalent) in THF. Inset: Job's plot curve of **BTPY** combined with Cu²⁺. The total concentration of **BTPY** and Cu²⁺ was 10 μ M. Excitation wavelength = 530 nm.

Ca²⁺, Ni²⁺, Ba²⁺, Mn²⁺, Au³⁺, Hg²⁺, Fe³⁺, Al³⁺, Ag⁺ and Cr³⁺. According to the results above, gradual attenuation in emission intensity during the fluorescence titration for Cu²⁺ by **BTPY** (10 μ M) was further confirmed (Fig. 2). The fluorescence intensity decreased by 100-fold until 1 equivalent of CuCl₂ was added to the solution of **BTPY** ($\Phi_{fl} = 0.3488$, in CH₂Cl₂), which is attributed to photo-induced electron transfer (PET) from the **BTPY** singlet excited state to the bound Cu²⁺ ion. Moreover, the characteristic emission band of **Cu(II)-BTPY** at 582 nm is blue-shifted by 10 nm compared to that of **BTPY**. To demonstrate the quenching procedure, the Job's plot curve was used for determining the complex stoichiometry (Fig. 2, Inset). Regular linear relationship between 1/(F₀ - F) and 1/[Cu²⁺] shows that **BTPY** is combined with Cu²⁺ for 1:1 with the binding constant

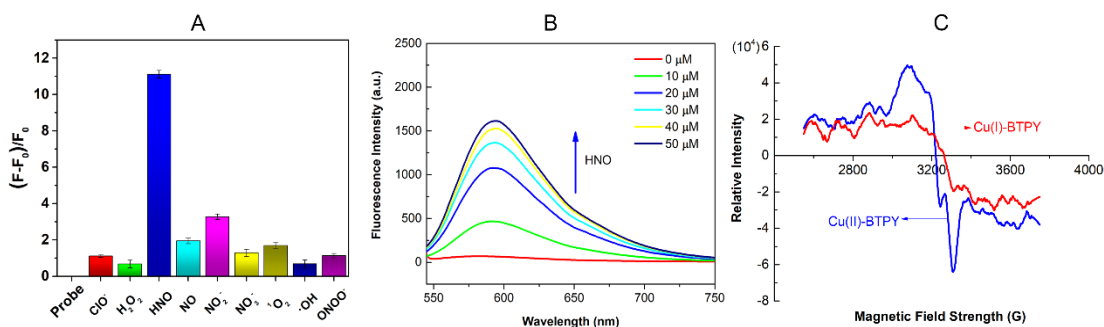


Fig. 3. (A) Fluorescence responses of **Cu(II)-BTPY** (10 μM) to various RNS and ROS analysis substances (1 mM of HNO (Angelis' salt), NO, H₂O₂, ClO⁻, ¹O₂, NO₂⁻, NO₃⁻, •OH and ONOO⁻ is the concentration of 0.1 mM, PBS buffer solution pH 7.4) in THF. F₀ represents the initial maximum emission intensity of **Cu(II)-BTPY**, F represents the final emission intensity of various ROS or RNS added to the probe **Cu(II)-BTPY**. The error bars represent the standard deviation. (B) Fluorescence responses of **Cu(II)-BTPY** (10 μM) to HNO analysis substances (1 mM of HNO (Angelis' salt) in THF. Excited wavelength = 530 nm. (C) EPR spectra recorded at 298 K for 0.5 mM **Cu(II)-BTPY** in aqueous DMSO (blue line) and with excess Angelis' salt (red line).

K_a equal to $3.2 \times 10^4 \text{ M}^{-1}$ that was calculated by the Benesi-Hildebrand equation (Fig. S2). In order to realize the fluorescent 'turn-on' performance upon HNO, Cu(II)-BTPY complex was prepared from the coordination of BTPY with CuCl₂ (Scheme 1), and certified by the positive ion electrospray mass spectrum suggesting a peak with *m/z* = 915.2206 that conforms to that of [Cu(II)-(BTPY)Cl]⁺ (calcd *m/z* = 915.2235) (Fig. S14).

Also, the responses of **Cu(II)-BTPY** to the reductive biological molecules were studied. Considering their importance in biological studies, reactive oxygen species (ROS) and reactive nitrogen species (RNS) (including NO, H₂O₂, ClO⁻, ¹O₂, NO₂⁻, NO₃⁻, •OH and ONOO⁻) were explored in comparison to HNO. As expected, **Cu(II)-BTPY** shows high selectivity toward HNO over relevant ROS and RNS species by measuring the respondent changes in the optical spectra while gradually adding consecutive amounts of ROS and RNS (Fig. 3A). Only the response of HNO displays the fluorescence enhancement in the **Cu(II)-BTPY** solution, as reflected by the emission color of solution turned from dark to bright pink (Fig. 4). The fluorescence response of others ROS and RNS such as NO, H₂O₂, ClO⁻, ¹O₂, NO₂⁻, NO₃⁻, •OH and ONOO⁻ is negligible. The difference of HNO from other ROS and RNS on **Cu(II)-BTPY** can be visually distinguished under UV light (Fig. 3D). As profiled in Fig. 3B, upon addition of 5 equiv HNO to **Cu(II)-BTPY**, the fluorescence increased gradually to a maximum at 592 nm with a simultaneous turned-on mode, implying that **Cu(II)-BTPY** was completely reduced by HNO. A typical paramagnetism with a symmetric line with *g* equal to 2.09 given by electron paramagnetic resonance (EPR) measurement confirms the reduction of the **Cu(II)-BTPY** into Cu(I)-BTPY. Excessively introducing Angelis' salt into the **Cu(II)-BTPY** solution resulted in a rapid decrement in the EPR signal that owes much to the diamagnetism of the reduced Cu(I)-BTPY (Fig. 3C). The HNO sensing properties of **Cu(II)-BTPY** were further probed by fluorescence titration, indicating that **Cu(II)-BTPY** is an excellent candidate for highly selective turn-on sensor in HNO identification.



Fig. 4. The photo of Cu(II)-BTPY under ultraviolet lamp (365nm) after addition of different ROS and RNS.

Additionally, the biologically discernable ability of **Cu(II)-BTPY** was evaluated via fluorescence imaging towards HNO operated in cervical cancer HeLa cells. We incubated the cells

with **Cu(II)-BTPY** in DMSO accompanied by 5% CO₂ flowing at 37 °C for 30 minutes, and no change in emission intensity was observed for cultures to which Angelis' salt was not added (Fig. 5 A, B). The following treatment of these cells with 3 mM Angelis' salt led to an increment in fluorescence in red channel (Fig. 5 C, D). The dramatic changes ascertain the potential practicability of **Cu(II)-BTPY** for monitoring HNO in living cells. In addition, we used MTS analysis to study the cytotoxicity of different concentrations of Cu(II)-BTPY or BTPY via incubation with HeLa cells for 24 hours. The cell viability of Cu(II)-BTPY or BTPY was 87.2% or 89.3%, respectively (Fig. S15, Fig. S16). Ultimately, zebrafish embryos were employed for the staining study to prove the applicability of **BTPY** skeleton in the more complex organism. As shown in Fig. 5 E-H, incubated with 10 μM **BTPY** within 30 minutes, the imaged zebrafish embryos display bright red fluorescence.

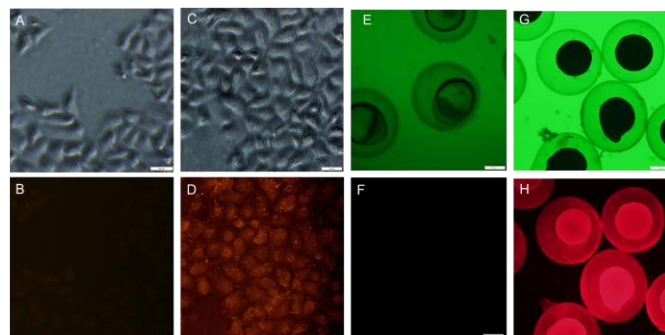


Fig. 5. HNO-induced fluorescence response in HeLa cells: (A, B) Images of cells stained with **Cu(II)-BTPY** (10 μM) in DMSO for 30 min at 37 °C. (C, D) Cells were incubated with **Cu(II)-BTPY** in DMSO for 30 min and then HNO (Angelis' salt) for 30 min at 37 °C. Scale bar, 50 μm ; Fluorescence images of probe **BTPY** in Zebrafish embryos: (E, F) Image of Zebrafish embryos stained without **BTPY** (10 μM) in DMSO for 30 min at 37 °C. (G, H) Image of Zebrafish embryos stained with **BTPY** (10 μM) in DMSO for 30 min at 37 °C. Scale bar, 200 μm . (A, C, E, G.) Bright field, (B, D, F, H) dark field. HeLa Cells and Zebrafish embryos images were obtained using an OLYMPUS IX71 inverted phase contrast fluorescence microscope.

Conclusions

In summary, we have described the design and synthesis of the turn-on reaction sensor on the basis of BODIPY-terpyridine-Cu(II) platform for highly selective detection of HNO over the other ROS and RNS species. It is worth mentioning that the relatively high fluorescence quantum efficiency and large Stokes shift of the sensor is useful for imaging experiments especially in living organisms. On the other hand, a series of transition metal ions were exploited, presenting Cu²⁺ as the optimal quenching

ion. EPR spectroscopic and ESI-MS studies showed that the sensing mechanism relies on reduction of Cu(II) by HNO. Moreover, the sensor Cu(II)-BODIPY has been successfully applied to monitoring and imaging of HNO in HeLa cells under physiological conditions. Thereby, it is considered that as-synthesized BTPY holds potential application prospect in dye behaviors in the living organisms.

Acknowledgments

This work was financially supported by NSFC (21462039, 51363019, 21761032). We thank Dr. Aihong Mao for her useful support and advices in cellular experiments.

Supplementary Material

Supplementary data associated with this article can be found in the online version at <http://dx.doi.org/10.xxxx/x.xxxx.xxxx.xx.xx>.

References

- (a) Green, S. J.; Crawford, R. M.; Hockmeyer, J. T.; Meltzer, M. S.; Nacy, C. A. *The Journal of Immunology*. **1990**, *145*, 4290-4297. (b) Zamora, R.; Vodovotz, Y.; Billiar, T. R. *Molecular Medicine*. **2000**, *6*, 347-373.
- (a) Fukuto, J. M.; Switzer, C. H.; Miranda, K. M.; Wink, D. A. *Annual review of pharmacology and toxicology*. **2005**, *45*, 335-355; (b) Fukuto, J. M.; Dutton, A. S.; Houk, K. N. *ChemBiochem: a European journal of chemical biology*. **2005**, *6*, 612-619; (c) Lopez, B. E.; Shinyashiki, M.; Han, T. H.; Fukuto, J. M. *Free radical biology & medicine*. **2007**, *42*, 482-491; (d) Paolucci, N.; Jackson, M. I.; Lopez, B. E.; Miranda, K.; Tocchetti, C. G.; Wink, D. A.; Hobbs, A. J.; Fukuto, J. M. *Pharmacology & therapeutics*. **2007**, *113*, 442-458.
- Miranda, K. M. *Coordination Chemistry Reviews*. **2005**, *249*, 433-455.
- Nazareno Paolucci, Tatsuo Katori, Hunter C. Champion, Marcus E. St. John, Katrina M. Miranda, Jon M. Fukuto, David A. Wink, and David A. Kass. *PNAS*. **2003**, *100*, 5537-5542.
- (a) Gao, W. D.; Murray, C. I.; Tian, Y.; Zhong, X.; DuMond, J. F.; Shen, X.; Stanley, B. A.; Foster, D. B.; Wink, D. A.; King, S. B.; van Eyk, J. E.; Paolucci, N. *Circulation research*. **2012**, *111*, 1002-1011; (b) Paolucci, N.; Saavedra, W. F.; Miranda, K. M.; Martignani, C.; Isoda, T.; Hare, J. M.; Espey, M. G.; Fukuto, J. M.; Feilisch, M.; Wink, D. A.; Kass, D. A. *Proceedings of the National Academy of Sciences of the United States of America*. **2001**, *98*, 10463-10468; (c) Sabbah, H. N.; Tocchetti, C. G.; Wang, M.; Daya, S.; Gupta, R. C.; Tunin, R. S.; Mazhari, R.; Takimoto, E.; Paolucci, N.; Cowart, D.; Colucci, W. S.; Kass, D. A. *Circulation. Heart failure*. **2013**, *6*, 1250-1258; (d) Sivakumaran, V.; Stanley, B. A.; Tocchetti, C. G.; Ballin, J. D.; Caceres, V.; Zhou, L.; Keceli, G.; Rainer, P. P.; Lee, D. I.; Huke, S.; Ziolo, M. T.; Kranias, E. G.; Toscano, J. P.; Wilson, G. M.; O'Rourke, B.; Kass, D. A.; Mahaney, J. E.; Paolucci, N. *Antioxidants & redox signaling*. **2013**, *19*, 1185-1197; (e) Switzer, C. H.; Flores, Santana, W.; Mancardi, D.; Donzelli, S.; Basudhar, D.; Ridnour, L. A.; Miranda, K. M.; Fukuto, J. M.; Paolucci, N.; Wink, D. A. *Biochimica et biophysica acta*. **2009**, *1787*, 835-840.
- Miao, Z.; King, S. B. *Nitric oxide: biology and chemistry*. **2016**, *57*, 1-14.
- (a) Cline, M. R.; Tu, C.; Silverman, D. N.; Toscano, J. P. *Free radical biology & medicine*. **2011**, *50*, 1274-1279; (b) Martí, M. A.; Bari, S. E.; Estrin, D. A.; Doctorovich, F. *Journal of the American Chemical Society*. **2005**, *127*, 4680-4684; (c) Suárez, S. A.; Martí, M. A.; Biase, P. M. de; Estrin, D. A.; Bari, S. E.; Doctorovich, F. *Polyhedron*. **2007**, *26*, 4673-4679; (d) Sulc, F.; Immoos, C. E.; Pervitsky, D.; Farmer, P. J. *Journal of the American Chemical Society*. **2004**, *126*, 1096-1101.
- (a) Ali, F.; Sreedharan, S.; Ashoka, A. H.; Saeed, H. K.; Smythe, C. G. W.; Thomas, J. A.; Das, A. *Analytical chemistry*. **2017**, *89*, 12087-12093; (b) Gong, X. Y.; Yang, X. F.; Zhong, Y. G.; Chen, Y. H.; Li, Z. *Dyes and Pigments*. **2016**, *131*, 24-32; (c) Kondapa Naidu Bobba, Ying Zhou, Lin E Guo, Tie Nan Zang, Jun Feng Zhang, and Sankarprasad Bhuniya. *RSC Adv*. **2015**, *5*, 84543-84546; (d) Tan, Y.; Liu, R. C.; Zhang, H. T.; Peltier, R.; Lam, Y. W.; Zhu, Q.; Hu, Y.; Sun, H. Y. *Scientific reports*. **2015**, *5*, 16979; (e) Rivera, Fuentes, P.; Lippard, S. J. *Accounts of chemical research*. **2015**, *48*, 2927-2934.
- (a) Sun, W.; Fan, J.; Hu, C.; Cao, J.; Zhang, H.; Xiong, X.; Wang, J.; Cui, S.; Sun, S. and Peng, X. *Chemical communications*. **2013**, *49*, 3890-3892; (b) Sun, W.; Guo, S.; Hu, C.; Fan, J. and Peng, X.; *Chemical Reviews*. **2016**, *116*, 7768-7817.
- (a) Zhou, B.; Qin, S.; Chen, B.; Han, Y. *Tetrahedron Letters*. **2018**, *59*, 4359-4363; (b) Kilic, B.; Yesilgul, N.; Polat, V.; Gercek, Z.; Akkaya, E. U. *Tetrahedron Letters*. **2016**, *57*, 1317-1320; (c) Ekmekci, Z. *Tetrahedron Letters*. **2015**, *56*, 1878-1881; (d) Cheng, D.; Zhao, W.; Yang, H.; Huang, Z.; Liu, X.; Han, A. *Tetrahedron Letters*. **2016**, *57*, 2655-2659; (e) Yan, Z.; Lin, X.; Guo, H.; Yang, F. *Tetrahedron Letters*. **2017**, *58*, 3064-3068; (f) Li, M.; Tian, R.; Fan, J.; Du, J.; Long, S.; Peng, X. *Dyes and Pigments*. **2017**, *147*, 99-105; (g) Loudet, A.; Burgess, K. *Chemical Reviews*. **2007**, *107*, 4891-4932.
- (a) Chen, B.; Fu, H.; Lv, Y.; Li, X.; Han, Y. *Tetrahedron Letters*. **2018**, *59*, 1116-1120; (b) Niu, L. Y.; Guan, Y. S.; Chen, Y. Z.; Wu, L. Z.; Tung, C. H.; Yang, Q. Z. *Journal of the American Chemical Society*. **2012**, *134*, 18928-18931; (c) Fan, J.; Mu, H.; Zhu, H.; Du, J.; Jiang, N.; Wang, J.; Peng, X. *Ind. Eng. Chem. Res.* **2015**, *54*, 8842-8846.
- (a) Agarwalla, H.; Mahajan, P. S.; Sahu, D.; Taye, N.; Ganguly, B.; Mhaske, S. B.; Chattopadhyay, S.; Das, A. *Inorganic chemistry*. **2016**, *55*, 12052-12060; (b) Bañuelos, J. *The Chemical Record*. **2016**, *16*, 335-348; (c) Boens, N.; Verbelen, B.; Dehaen, W. *Eur. J. Org. Chem.* **2015**, *2015*, 6577-6595; (d) Xu, J.; Zhang, Y.; Yu, H.; Gao, X.; Shao, S. *Analytical chemistry*. **2016**, *88*, 1455-1461;
- (a) Arranja, C. T.; Aguiar, A.; Encarnação, T.; Fonseca, S. M.; Justino, L. L.G.; Castro, R. A.E.; Benniston, A.; Harriman, A.; Burrows, H. D.; Sobral, A. J.F.N. *Journal of Molecular Structure*. **2017**, *1146*, 62-69; (b) Chen, H.; He, X.; Su, M.; Zhai, W.; Zhang, H.; Li, C. *Journal of the American Chemical Society*. **2017**, *139*, 10157-10163; (c) Ke, C. S.; Fang, C. C.; Yan, J. Y.; Tseng, P. J.; Pyle, J. R.; Chen, C. P.; Lin, S. Y.; Chen, J.; Zhang, X.; Chan, Y. H. *ACS nano*. **2017**, *11*, 3166-3177; (d) Kolemen, S.; Akkaya, E. U. *Coordination Chemistry Reviews*. **2018**, *354*, 121-134; (e) Vázquez, Romero, A.; Kielland, N.; Arévalo, M. J.; Preciado, S.; Mellanby, R. J.; Feng, Y.; Lavilla, R.; Vendrell, M. *Journal of the American Chemical Society*. **2013**, *135*, 16018-16021.
- (a) Bura, T.; Retailleau, P.; Ulrich, G.; Ziesse, R. *The Journal of organic chemistry*. **2011**, *76*, 1109-1117; (b) Huang, L.; Yu, X.; Wu, W.; Zhao, J. *Organic letters*. **2012**, *14*, 2594-2597; (c) Zhu, S. L.; Zhang, J. T.; Vegesna, G.; Tiwari, A.; Luo, F. T.; Zeller, M.; Luck, R.; Li, H. H.; Green, S.; Liu, H. Y. *RSC Adv*. **2012**, *2*, 404-407.
- (a) Uma, V.; Kanthimathi, M.; Weyhermuller, T.; Nair, B. U. *Journal of inorganic biochemistry*. **2005**, *99*, 2299-2307; (b) Zhao, L. X.; Kim, T. S.; Ahn, S. H.; Kim, T. H.; Kim, E. k.; Cho, W. J.; Choi, H.; Lee, C. S.; Kim, J. A.; Jeong, T. C.; Chang, C. j.; Lee, E. S. *Bioorganic & Medicinal Chemistry Letters*. **2001**, *11*, 2659-2662.
- (a) Apfel, U. P.; Buccella, D.; Wilson, J. J.; Lippard, S. J. *Inorganic chemistry*. **2013**, *52*, 3285-3294; (b) Wrobel, A. T.; Johnstone, T. C.; Deliz Liang, A.; Lippard, S. J.; Rivera-Fuentes, P. *Journal of the American Chemical Society*. **2014**, *136*, 4697-4705; (c) Zhou, Y.; Liu, K.; Li, J. Y.; Fang, Y.; Zhao, T. C.; Yao, C. *Organic letters*. **2011**, *13*, 1290-1293.
- Tan, Y.; Liu, M.; Gao, J.; Yu, J.; Cui, Y.; Yang, Y.; Qian, G. *Dalton Trans*. **2014**, *43*, 8048-8053.



A Cu(II)-BODIPY was rationally designed and synthesized as a reducing reaction turn-on fluorescent probe for HNO over ROS and RNS species.

6

Tetrahedron

- A turn-on mode targeted fluorescent sensor design strategy
- Significant stokes shift and relatively high fluorescence quantum efficiency
- Highly selective determination of HNO over ROS and RNS species based on reducing reaction
- Potential approach to bioimaging in vivo

ACCEPTED MANUSCRIPT